



Seakeeping Analysis of a Hydrofoil Supported Watercraft (Hysuwac): A Case Study

Ketut Suastika^{1,*}, Agung Silaen¹, Muhammad Hafiz Nurwahyu Aliffrananda¹, Yuda Apri Hermawan¹

¹ Department of Naval Architecture, Faculty of Marine Technology, Institut Teknologi Sepuluh Nopember (ITS), Surabaya 60111, Indonesia

ARTICLE INFO

Article history:

Received 21 May 2021

Received in revised form 29 May 2021

Accepted 30 May 2021

Available online 31 May 2021

Keywords:

Energy efficiency; Hysuwac; NORDFORSK criteria; Panel method; Seakeeping characteristics

ABSTRACT

Considering recent global temperature increase and observed climate change, efforts have been made towards energy efficiency and reduction of green-house gas emission. A foil system is proposed in this study and retrofitted to an existing catamaran to reduce the energy use and to improve the vessel's seakeeping characteristics. The objective of this study is to investigate the effects of the application of the foil system on the seakeeping performance of the vessel. CFD simulations based on a panel method were carried out to obtain the seakeeping characteristics of the catamaran with and without foil system. Simulation results show that the foil system reduced the vessel motions in a seaway: the heave-, pitch- and roll significant amplitudes were reduced 4.41, 9.97 and 3.30 percent, respectively, due to the application of the foil system. In addition, the vertical accelerations at the fore perpendicular (FP) and at deck were reduced 3.66 and 9.70 percent, respectively. A check against the NORDFORSK criteria for fast small crafts shows that the vessel can operate safely up to sea state 2.

1. Introduction

Hydrofoil supported watercrafts (hysuwac) are catamarans utilized with a foil system, consisting of a fore foil, placed some distance forward the center of gravity, and an aft foil placed near the stern. Compared to monohull vessels, catamarans have the advantages of having a larger deck space and a better transverse stability. Another advantage is that catamarans have less resistance compared to similar monohull ships. This makes catamarans widely used as fast boats for military purposes as well as passenger ships with short to medium shipping distances [1]. The principal disadvantage of catamarans compared to monohull ships is that high-speed catamarans generally have poor seakeeping quality in rough water [2].

The application of a foil system to a catamaran may offer a more efficient use of energy by lowering the propulsion power compared to a similar deep V monohull and a resistance characteristic improvement compared to fast catamarans that do not use hydrofoils [3,4]. The pioneering works on research and development of hydrofoil supported catamarans (hysucat) and hydrofoil supported watercrafts (hysuwac) were attributed to Prof. K. G. Hoppe at the university of Stellenbosch, Republic of South Africa, who initiated the study in the end of 1970s or the beginning of 1980s [5,6]. Beside

* Corresponding author

E-mail address: k_suastika@na.its.ac.id (Ketut Suastika)

propulsion power reduction, the application of a hydrofoil system to a catamaran can result in better seakeeping characteristics in rough water [3]. The hydrofoil system was also found to reduce the vessel's vertical acceleration [7].

The hydrodynamic performance of a hysucat or a hysuwac was reported to depend on the hydrofoils used. Najafi *et al.*, [8] studied experimentally the seakeeping performance of a hydrofoil supported catamaran (hysucat) utilizing three different types of hydrofoils, namely NACA 16, EPPLER 874 and Gottingen 11k, and found that the Gottingen 11k performed best. However, other studies reported by Suastika *et al.*, [9] and Riyadi and Suastika [10] found that NACA 64₁-212 gave an adequate hydrodynamic performance for these purposes. Beside the foil type, the hydrodynamic performance of the hysucat or hysuwac also depends on the placing of the hydrofoils relative to the catamaran and the magnitude of the generated foil lift relative to the vessel displacement. Therefore, a proper arrangement should be designed prior to the application of the foil system. These aspects are still insufficiently reported in the literature of hydrofoil applications to catamarans.

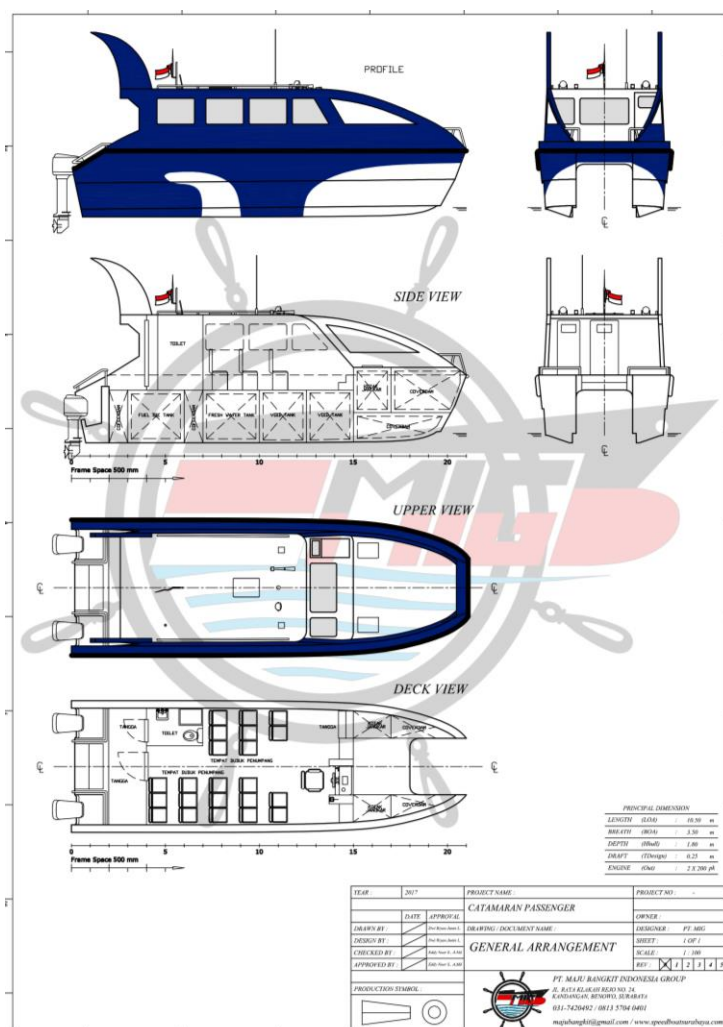


Fig. 1. General arrangement of the 10.5-m catamaran considered in this study

The central question in this study is whether a retrofit of a foil system to an existing catamaran can improve the seakeeping characteristics of the vessel. A 10.5-m passenger catamaran with a service speed $V_s = 24.5$ knots ($Fr = 1.24$) is considered, which was designed and built by PT. Maju Bangkit Indonesia Group, Surabaya, Indonesia. The vessel's general arrangement is shown in Figure

1 and its main particulars are tabulated in Table 1. A foil system arrangement is proposed as shown in Figure 2. Figure 2 indicates the position of the hydrofoils in the longitudinal direction and their submerged position below the water surface. This configuration is called a hydrofoil supported watercraft (hysuwac) [4]. The foils submerged depth was determined from $h/c = 0.4$, where h is the submerged depth and c is the chord length of the hydrofoil [11]. The objective of the study is to investigate the effects of the foil system on the seakeeping characteristics of the vessel.

Table 1
 Main particulars of the vessel

Parameter	Unit	Value
Length overall (LOA)	m	10.50
Breadth (B)	m	3.50
Height (H)	m	1.80
Draft (T)	m	0.25
Block coefficient of a demihull (C_B)	-	0.25
Longitudinal centre of gravity measured from AP (LCG)	m	4.18
Total displacement (Δ)	ton	1.965
Service speed (V_s)	kn	24.5

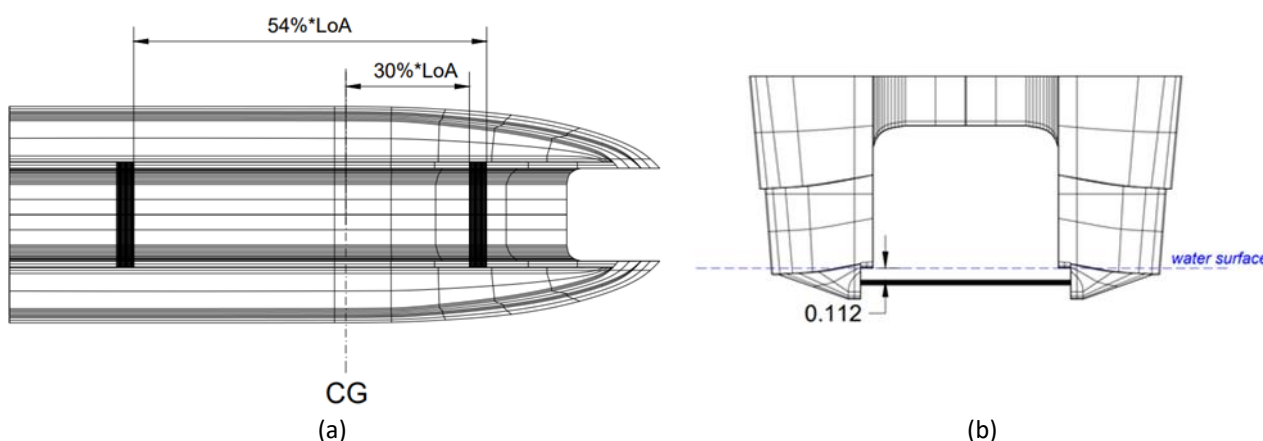


Fig. 2. Plan and aft views of the hydrofoil supported watercraft (hysuwac): (a) position of the hydrofoils in the longitudinal direction and (b) the submerged depth of the hydrofoils

2. Methodology

A computational fluid dynamics (CFD) method is utilized in this study. The motion modes considered are heave, pitch, and roll, which are most significant for the passenger comfort and vessel's seakeeping quality. Data of the hydrofoils and sea condition are presented below, followed by a presentation of the CFD method to calculate the vessel's response amplitude operators (RAOs). Based on the RAOs and the wave spectrum, the response spectra for the heave-, pitch- and roll motions are determined, and the response statistics are calculated. To evaluate the seakeeping quality, the vertical accelerations at the fore perpendicular (FP) and at deck are calculated and, together with the roll angle, are checked against the NORDFORSK criteria for fast small crafts [12].

2.1 Data of the Hydrofoils and Sea Condition

Based on the studies reported by Saputro and Suastika [13], Suastika *et al.*, [9] and Riyadi and Suastika [10], both the fore and aft hydrofoils shown in Figure 2 are NACA 64₁-212 [14]. The span s is equal to the distance between the demihulls (1.7 m) and the chord length c was obtained by requiring a total foils lift of 40% of the vessel displacement, accounting a 10% lift reduction due to the disturbing effects of the demihulls on the water flow [15]. (The effective design lift is 30% of the vessel's displacement.) The foil aspect ratio $A = s/c = 6.07$. Furthermore, the foils angle of attack was fixed at $\mu = 4^\circ$ relative to the horizontal plane, which corresponds to the maximum value of lift to drag ratio [16]. All these parameters are summarized in Table 2.

Table 2
 Dimensions of the hydrofoils with optimum angle of attack

Parameter	Unit	Value
Chord length	m	0.28
Span	m	1.7
Aspect ratio	-	6.07
Planform area	m ²	0.476
Optimum angle of attack	deg	4.0

In addition to the vessel and hydrofoil geometrical data, data of the sea condition in the operating area and data of vessel's radii of gyration must be provided for the seakeeping simulations. These data are summarized as follows:

- a) Sea condition in the operating area:
 - Location: Labuan Bajo, Greater Sunda Islands, Indonesia (see Figure 3). The sea around Labuan Bajo, zoomed in from Figure 3, is shown in Figure 4. The significant wave height in this area is $H_s = 0.5$ m (see Figure 5) [17].
 - Water depth: 31.5 m
 - Water density: 1025 kg/m³

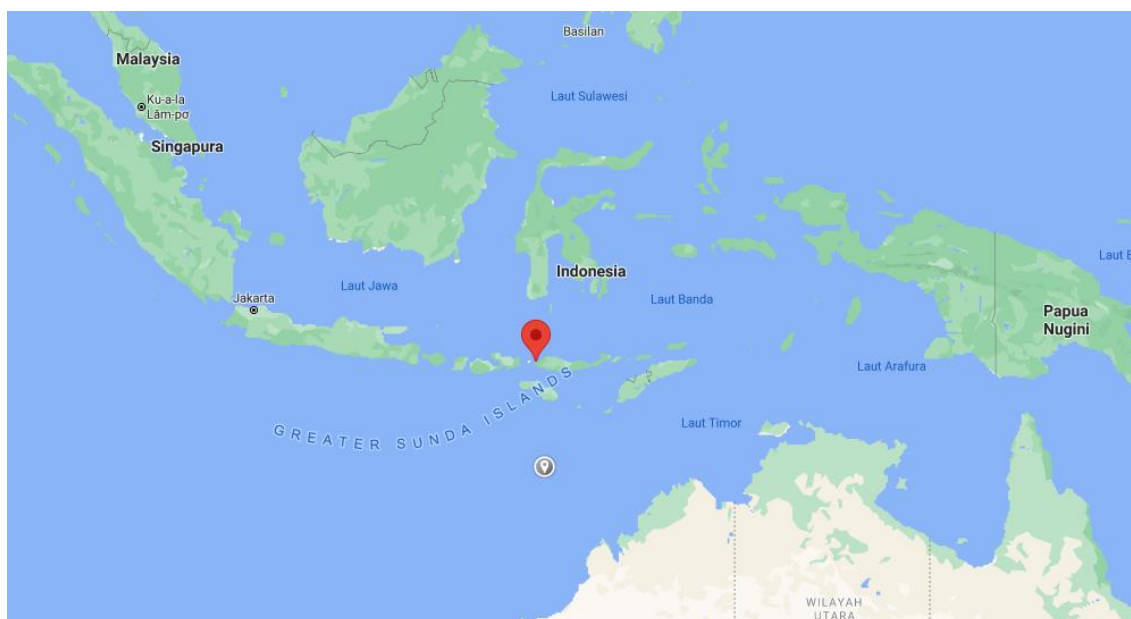


Fig. 3. A map showing the Indonesian archipelago with the location of Labuan Bajo (red balloon)

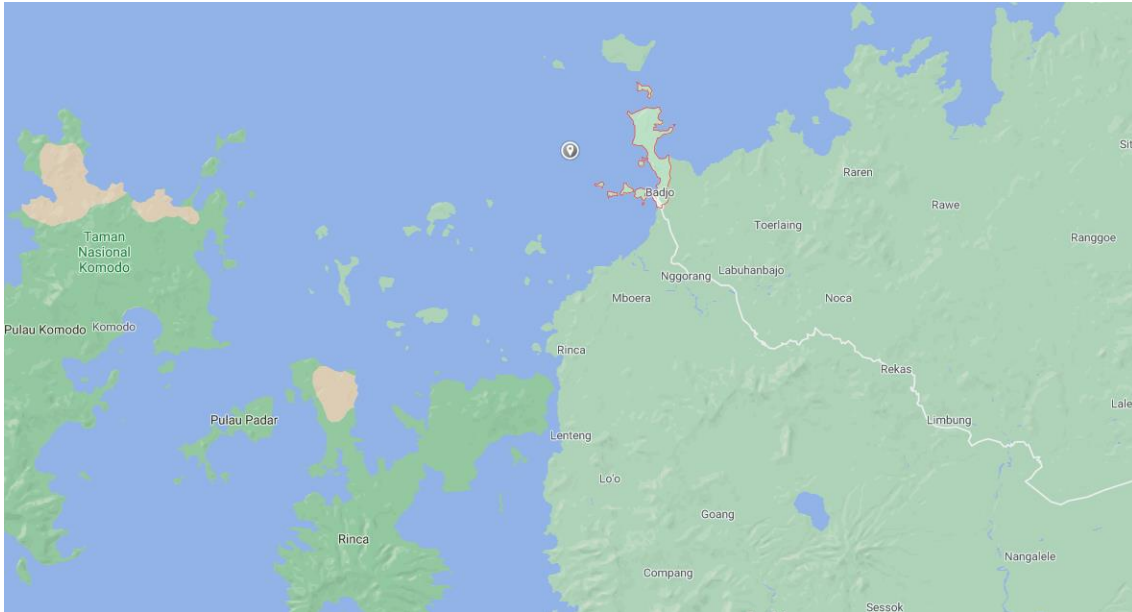


Fig. 4. The sea around Labuan Bajo (zoomed in from Figure 3)

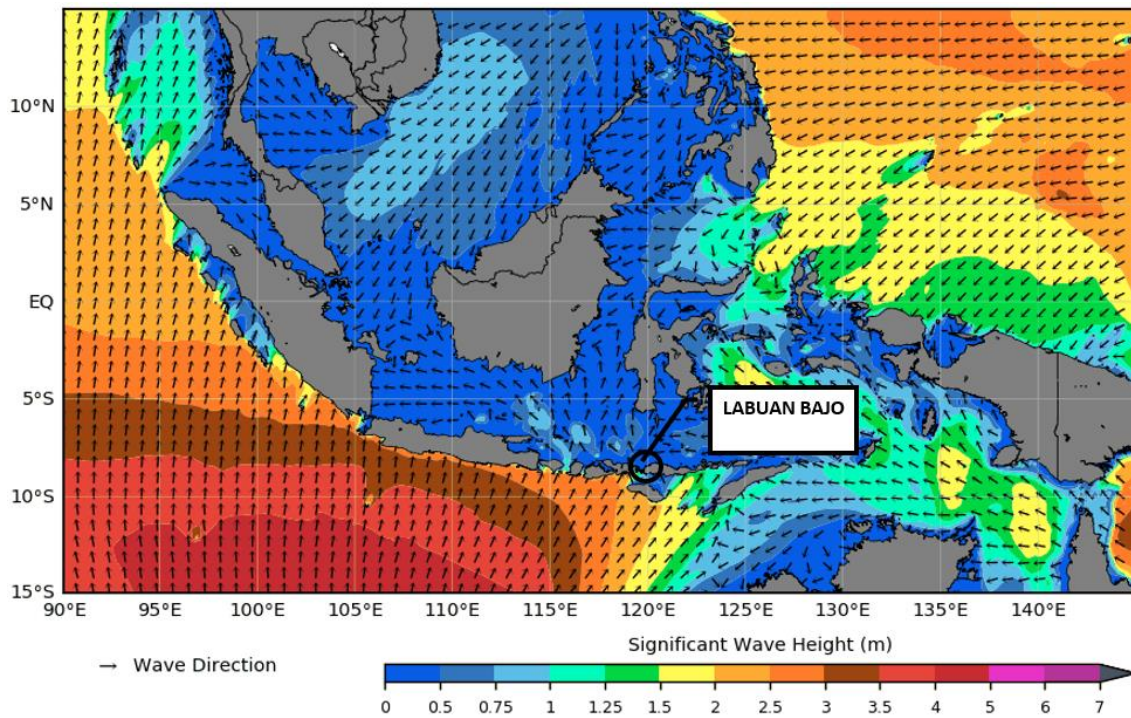


Fig. 5. A chart of significant wave height and wave direction in the Indonesian waters [17]

b) Vessel's radii of gyration are tabulated in Table 3.

Table 3
 Radii of gyration of the vessel

Component	Without hydrofoil	With hydrofoils
K_{xx} [m]	1.411	1.376
K_{yy} [m]	2.859	2.845
K_{zz} [m]	2.487	2.490

2.2 Representation of the Sea Condition

The sea condition in the vessel's operating area is represented by the ITTC wave spectrum, which is given by the following expression [18]:

$$S_{\zeta}(\omega) = \frac{0.0081g^2}{\omega^5} \exp\left(-\frac{3.11}{H_s^2 \omega^4}\right) \quad (1)$$

where $S_{\zeta}(\omega)$ is the wave spectral density, ω is the wave frequency, H_s is the significant wave height and g is the gravitational acceleration. For a vessel sailing with a speed V_s and a heading angle μ relative to the wave propagation direction, the encounter wave frequency ω_e due to the Doppler shift is given as [19]:

$$\omega_e = \omega \left(1 - \frac{\omega V_s}{g} \cos \mu\right) \quad (2)$$

The heading angles considered in this study are $\mu = 90^\circ$, 135° and 180° (beam sea, bow quartering sea and head sea, respectively). Furthermore, the wave spectral density as function of the encounter wave frequency ω_e is given as follows [19]:

$$S_{\zeta}(\omega_e) = S_{\zeta}(\omega) \frac{1}{1 - (2\omega V_s / g) \cos \mu} \quad (3)$$

where $S_{\zeta}(\omega)$ is the wave spectrum given by Eq. (1), ω is the wave frequency, V_s is the vessel's speed, μ is the heading angle and g is the gravitational acceleration.

Figure 6(a) shows the ITTC wave spectra for sea states 2 and 3 ($H_s = 0.5$ and 1.25 m, respectively) while Figure 6(b) shows the corresponding spectra based on the encounter wave frequency for vessel's speed $V_s = 24.5$ knots and a heading angle $\mu = 180^\circ$ (head waves). Due to the vessel's speed and the heading angle, the encounter wave frequency increases but the spectral density decreases in this case. However, the area under the spectral density curves remains unchanged either using a description based on the wave frequency ω or encounter wave frequency ω_e .

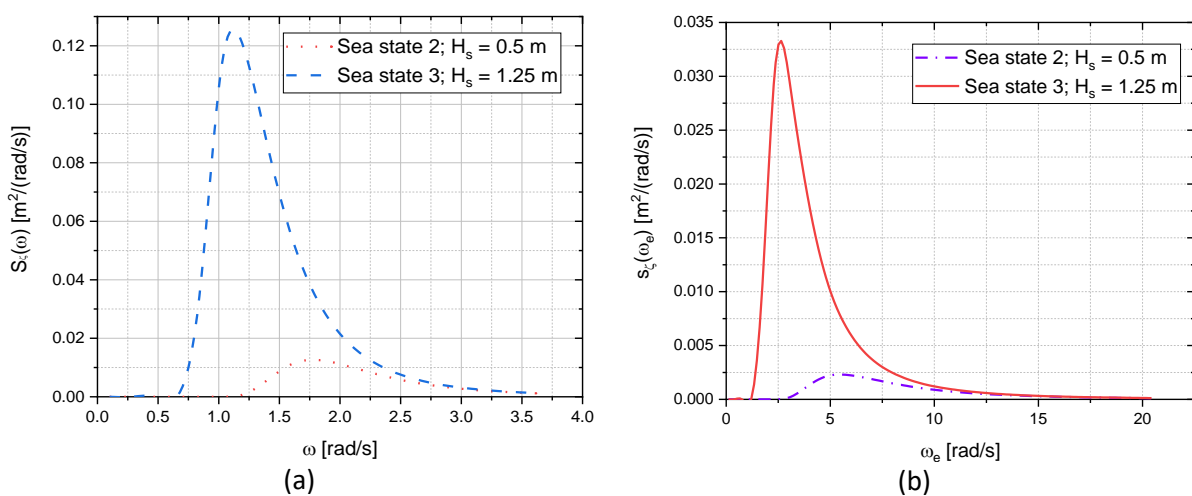


Fig. 6. Wave spectrum: (a) based on the wave frequency ω and (b) based on the encounter wave frequency ω_e for vessel's speed of 24.5 knots and heading angle of 180° (head waves)

2.3 CFD Simulations of Vessel Motions in a Seaway

CFD simulations based on a panel method were carried out utilizing Ansys Aqwa [20] to simulate the coupled six-degrees of freedom motion of the vessel in a seaway. Three dimensional (3D) models of the hull with and without foils were generated with the aid of the Maxsurf Modeller by Bentley [21], utilizing data of the vessel’s lines plan and the foil geometry. To ensure that the numerical model represents the prototype accurately, the hydrostatic data of the numerical model were verified using the prototype hydrostatic data. Table 4 summarizes the verification results for the case of catamaran without foil system. As shown in Table 4, the differences between the 3D model results and the prototype hydrostatic data are less than 2% for all parameters considered, indicating accurate geometrical modeling results. The 3D model generated by the Maxsurf Modeller was then exported in a .igs (dot igs) file format and then imported to Ansys Aqwa. The result for the case of catamaran without foil is shown in Figure 7.

Table 4

Comparison between the 3D numerical model and prototype hydrostatic data

Parameter	3D numerical model	Prototype data	Difference [%]
Displacement Δ [ton]	1.987	1.965	1.107
Draft T [m]	0.250	0.250	0.000
Length of Waterline LWL [m]	9.660	9.690	0.310
Prismatic coefficient C_p	0.856	0.853	-0.352
Block coefficient C_B	0.250	0.250	0.000
Midship coefficient C_M	0.292	0.287	-1.742
Longitudinal center of buoyancy, measured from AP, LCB [m]	4.193	4.189	-0.095

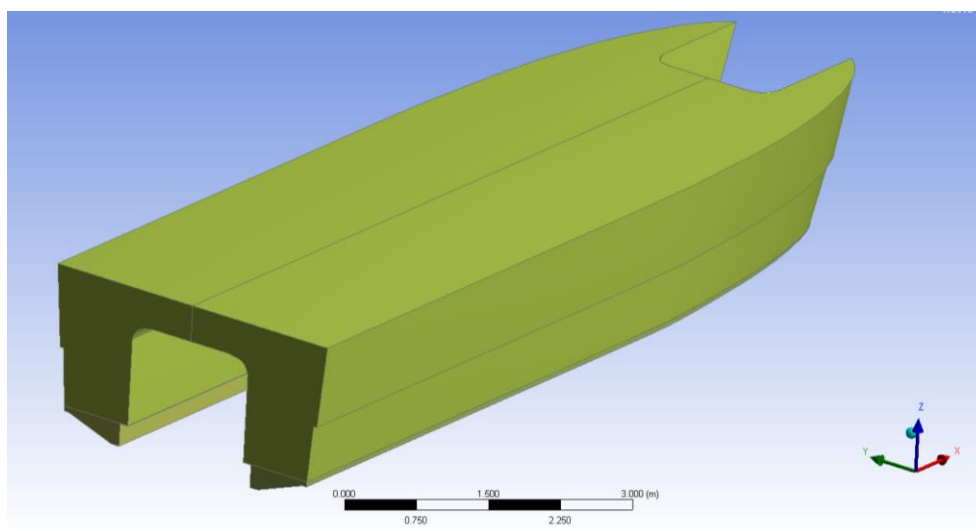


Fig. 7. 3D model of the catamaran without foil system

A computational domain was defined as shown in Figure 8 with dimensions as follows [20]: $X = 10$ LOA (105 m), $Y = 4.5$ LOA (47.25 m) and $Z =$ the water depth (31.5 m). The hull and foil surfaces were meshed as shown in Figure 9. Grid independence tests were carried out to determine the optimum number of cells (elements) used in the final setting of the simulations (see Section 3). The other input parameters for the simulations are the wave heading, vessel’s speed, and frequency interval for the discretization of the wave spectrum.

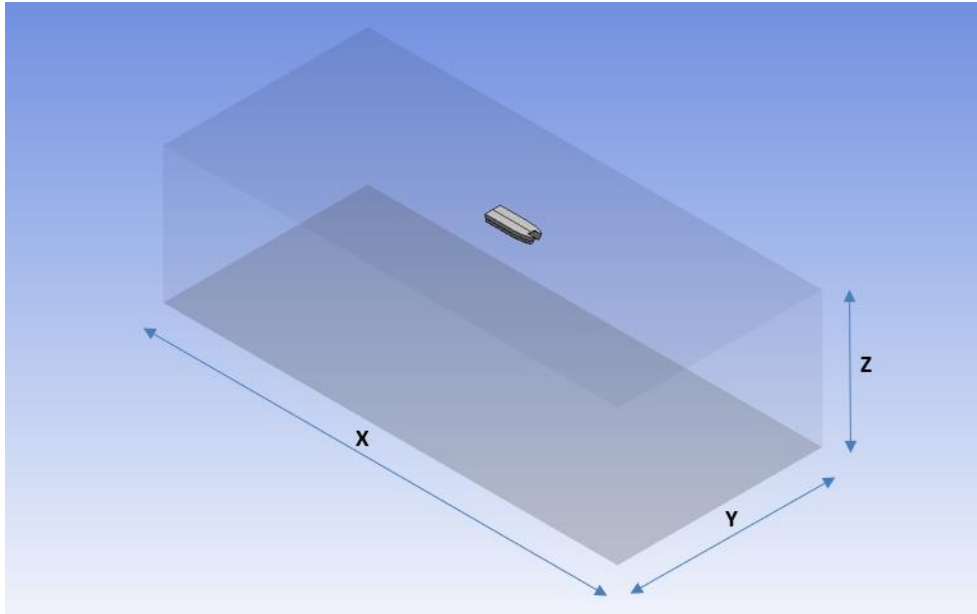


Fig. 8. Dimensions of the computational domain with the vessel therein

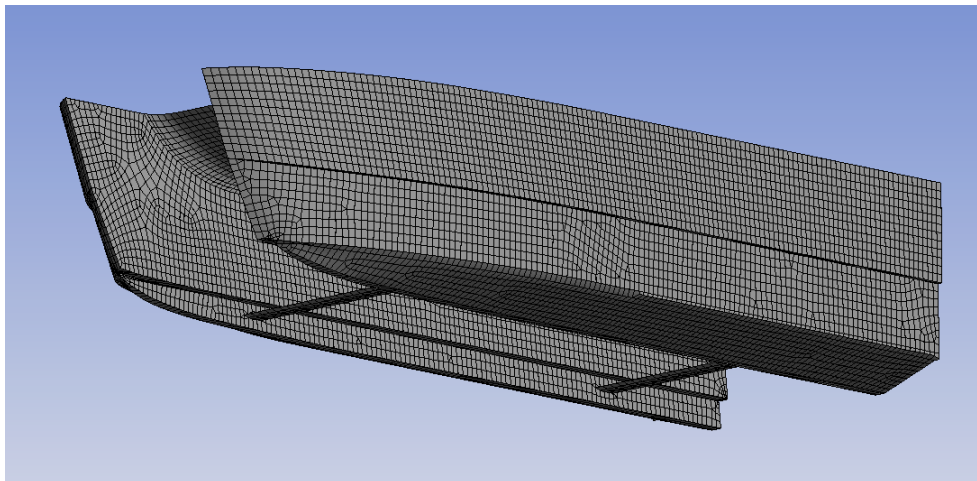


Fig. 9. A mesh of the catamaran with foil system (hysuwac)

2.4 Calculation of Response Spectra and Statistics

Utilizing the response amplitude operator (RAO) and the wave spectrum $S_{\zeta}(\omega_e)$, the response spectrum $S_r(\omega_e)$ is calculated as follows [19]:

$$S_r(\omega_e) = [\text{RAO}(\omega_e)]^2 S_{\zeta}(\omega_e) \quad (4)$$

For vessel at zero speed the encounter wave frequency is equal to the wave frequency ($\omega_e = \omega$). In addition to the heave, pitch and roll responses, the vertical accelerations at the fore perpendicular (FP) and at the deck were also calculated for the purpose of ship operability analysis. To calculate the vertical accelerations, first, the relative motion spectra at FP and at deck are calculated using the following formula [19]:

$$S_s(\omega_e) = S_z(\omega_e) + [xS_{\theta}(\omega_e)] - S_{\zeta}(\omega_e) \quad (5)$$

where $S_s(\omega_e)$ is the relative motion spectrum, $S_z(\omega_e)$ the heave spectrum, $S_\theta(\omega_e)$ is the pitch spectrum, $S_\zeta(\omega_e)$ is the wave spectrum and x is the longitudinal distance from the centre of gravity (CG) to the point under consideration. Based on the relative motion spectrum, the velocity and acceleration spectra are calculated as follows:

$$S_v(\omega_e) = \omega_e^2 S_s(\omega_e) \quad (6)$$

$$S_a(\omega_e) = \omega_e^4 S_s(\omega_e) \quad (7)$$

where $S_v(\omega_e)$ is the velocity spectrum and $S_a(\omega_e)$ is the acceleration spectrum.

As response statistics, the rms and significant amplitude of the responses are calculated. The rms value is calculated as $\sqrt{m_0}$ and the significant amplitude as $2\sqrt{m_0}$, where m_0 is the area under the response curve. Results of the vessel's RAOs, response spectra and response statistics are presented in Section 4.

3. Grid Independence Tests

Grid independence tests were carried out to verify the convergence of the numerical calculations and to determine the optimum number of elements to be used in the final setting of the CFD simulations. The heave and roll RAOs were considered in these tests for the case of catamaran without foil system at zero speed and under the heading angle of 90° . The area under the RAO curves was calculated as function of number of elements used in the simulations. The results are tabulated in Table 5 and plotted in Figure 10. Figure 10(a) shows that, for the heave motion, there are some oscillations in the value of the area under the RAO curve with increasing number of elements in the simulations. It starts with a decrease, followed by an increase and then, again a decrease, before it reaches an asymptotic end value. Further, Figure 10(b) shows that the area under the roll RAO also exhibits some variations before reaching an asymptotic end value.

Based on the results tabulated in Table 5 and shown in Figure 10, the number of elements of 23,131 is considered as the optimum number of elements for the final simulations. An increase of element number above 23,131 would result in practically no difference of the area under the RAO curves for both the heave and roll motions.

Table 5
Grid independence tests for the seakeeping simulations

Maximum element size	Number of elements	Heave Area [m.rad/(m.s)]	Difference [%]	Roll Area [deg.rad/(m.s)]	Difference [%]
0.41	3,069	2.264		94.442	
0.29	6,296	2.259	-0.221	92.586	-1.965
0.18	12,920	2.260	0.044	92.775	0.204
0.13	23,131	2.259	-0.044	92.897	0.132
0.10	36,356	2.259	0.000	92.892	-0.005

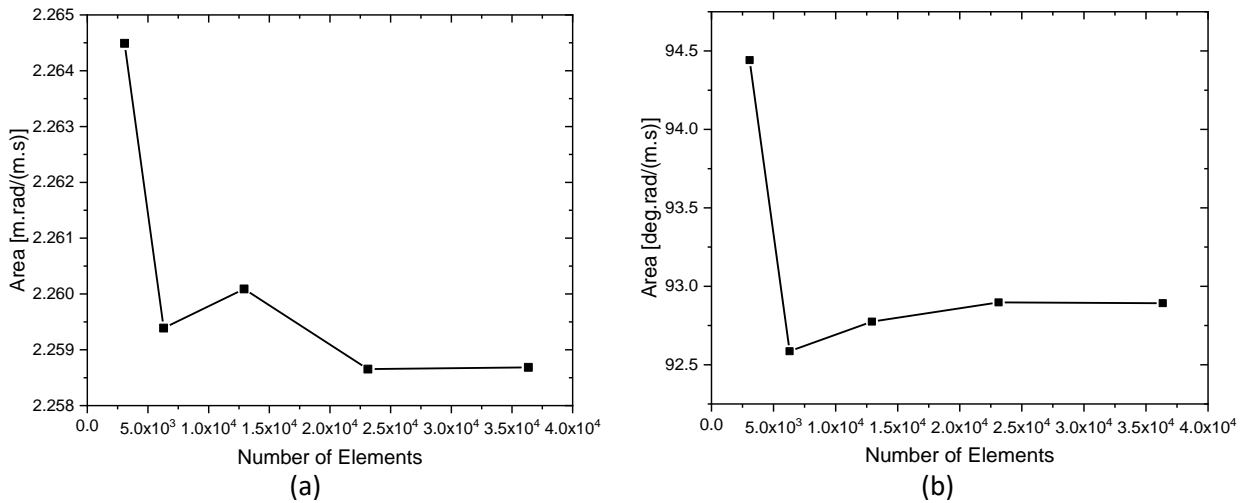


Fig. 10. Area under the RAO curves calculated using an increasing number of elements in the simulations for zero-speed vessel and heading angle $\mu = 90^\circ$: (a) heave and (b) roll motion

Figure 11 shows the heave and roll RAOs of the vessel at zero speed calculated using 23,131 elements in the simulations with heading angles $\mu = 90^\circ, 135^\circ$ and 180° for the cases of catamaran with and without foil system. Figure 11 shows an increase in the heave response but a decrease in the roll response due to the application of the foil system. However, because the speed is zero, there would be no lift (and drag) generated by the foils. To study the effects of the foil system on the vessel’s seakeeping, it is more interesting to consider the case of a sailing vessel. In the following section, the seakeeping characteristics are presented for the vessel at service speed $V_s = 24.5$ knots ($Fr = 1.24$).

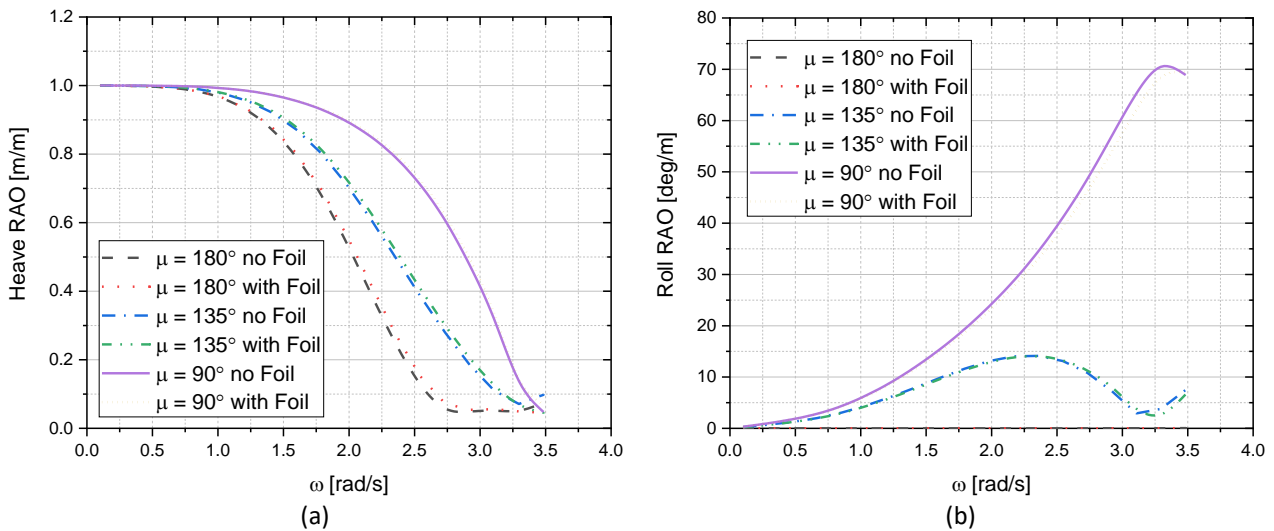


Fig. 11. Heave and roll RAOs for zero speed vessel calculated using 23,131 elements in the simulations

4. Results and Discussion

4.1 Response Amplitude Operators (RAOs)

Results of the seakeeping simulations for catamaran with and without foil system at service speed $V_s = 24.5$ knots ($Fr = 1.24$) are presented in this section. Figure 12 to Figure 14 show comparisons of the heave-, pitch- and roll RAOs, respectively, for the cases of catamaran with and without foil system. Figure 12 and Figure 13 show that the largest heave and pitch responses are for the wave

heading $\mu = 180^\circ$ (head sea), followed subsequently by $\mu = 135^\circ$ and 90° . For the roll motion, however, the largest response is for the wave heading $\mu = 90^\circ$ (beam sea), followed subsequently by $\mu = 135^\circ$ and 180° as shown in Figure 14. Further, the roll response at the wave heading $\mu = 180^\circ$ (head sea) is negligible. These observations are as expected.

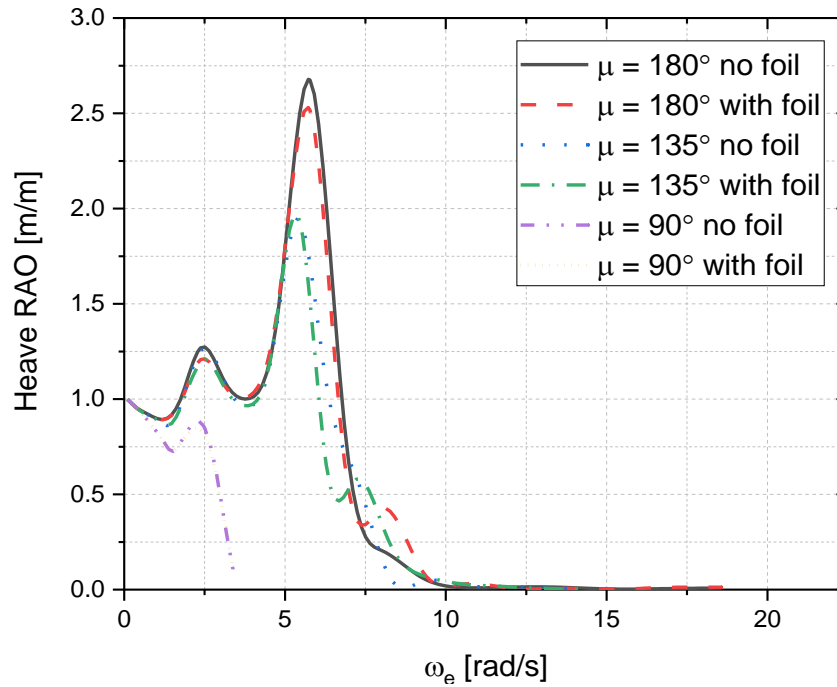


Fig. 12. Heave RAO for catamaran with and without foil system at service speed $V_s = 24.5$ knots ($Fr = 1.24$) in sea state 2 ($H_s = 0.5$ m)

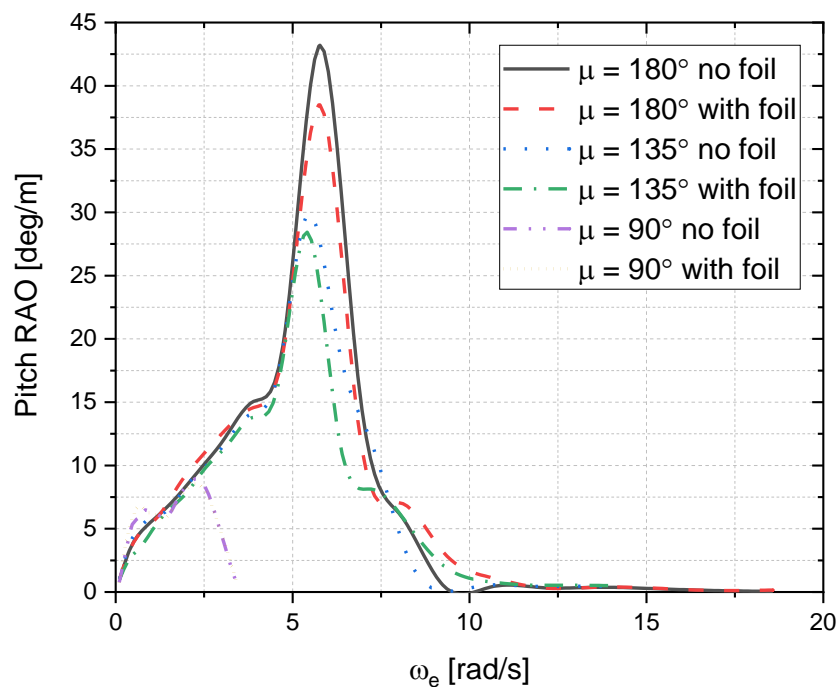


Fig. 13. Pitch RAO for catamaran with and without foil system at service speed $V_s = 24.5$ knots ($Fr = 1.24$) in sea state 2 ($H_s = 0.5$ m)

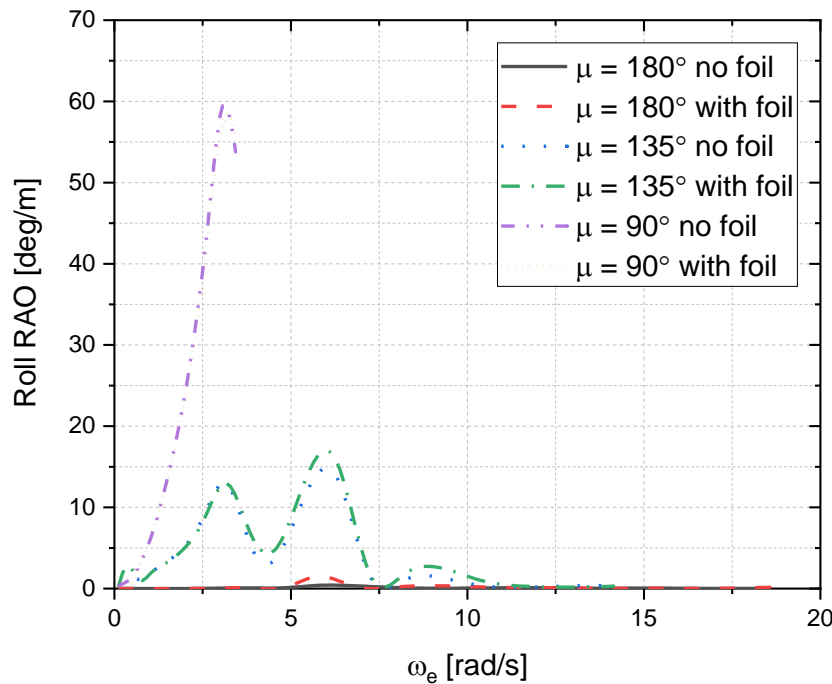


Fig. 14. Roll RAO for catamaran with and without foil system at service speed $V_s = 24.5$ knots ($Fr = 1.24$) in sea state 2 ($H_s = 0.5$ m)

Figure 12 to Figure 14 show that the application of the foil system generally reduced the vessel's motions. A clear reduction was observed for the heave and pitch responses at wave headings $\mu = 180^\circ$ and 135° . No significant reduction was observed for the roll motion due to the foil system. To quantify these effects, the response spectra and statistics were calculated and are presented in the following subsection.

4.2 Response Spectra and Statistics

Typical response spectra are shown in Figure 15 to Figure 17 for the heave- pitch- and roll motions, respectively in sea state 2 ($H_s = 0.5$ m). The vessel speed $V_s = 24.5$ knots ($Fr = 1.24$). In these figures, the responses of the catamaran without foil system are compared with those with foil system. Figure 15 and Figure 16 show a significant reduction in the heave and pitch motions for wave heading $\mu = 180^\circ$ due to the application of the foil system. In addition, a reduction in roll motion is observed for wave heading $\mu = 90^\circ$ due to the foil system (see Figure 17). The roll motion for $\mu = 180^\circ$ is negligible.

To quantify the above effects, the significant amplitudes of the heave-, pitch- and roll motions were calculated, and the results are tabulated in Table 6 to Table 8. Table 6 and Table 7 show that the heave and pitch significant amplitudes decreased due to the application of the foil system for all wave headings considered. The largest decrease of heave amplitude was observed for wave heading $\mu = 180^\circ$ with a value of 4.41 percent, followed subsequently by wave headings 135° and 90° with values 3.25 and 2.13 percent, respectively. The largest decrease of pitch amplitude is 9.97% for wave heading $\mu = 180^\circ$, followed subsequently by wave headings 135° and 90° with values 9.63 and 2.70 percent, respectively.

Table 8 shows that the significant roll amplitude decreases 3.30 percent for wave heading 90° but increases 13.64 percent for wave headings 135° due to the application of the foil system. However, the roll significant amplitudes for wave headings 135° and 180° are much smaller than that for wave

heading 90° . The reduction of heave-, pitch- and roll amplitudes due to the application of a foil system is in accordance with the results reported by Hoppe [3].

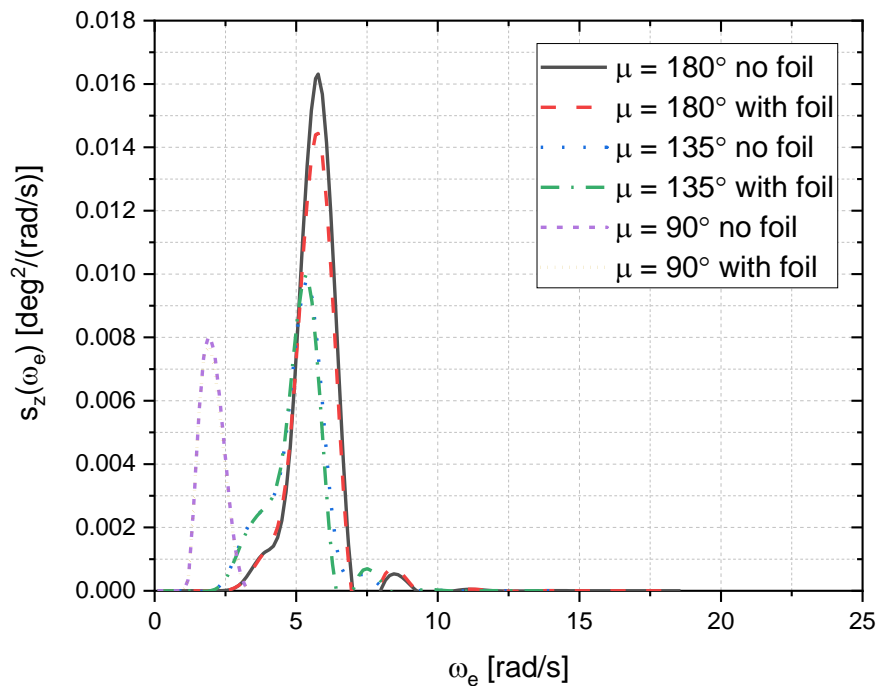


Fig. 15. Heave spectra for catamaran with and without foil system at service speed $V_s = 24.5$ knots ($Fr = 1.24$) in sea state 2 ($H_s = 0.5$ m)

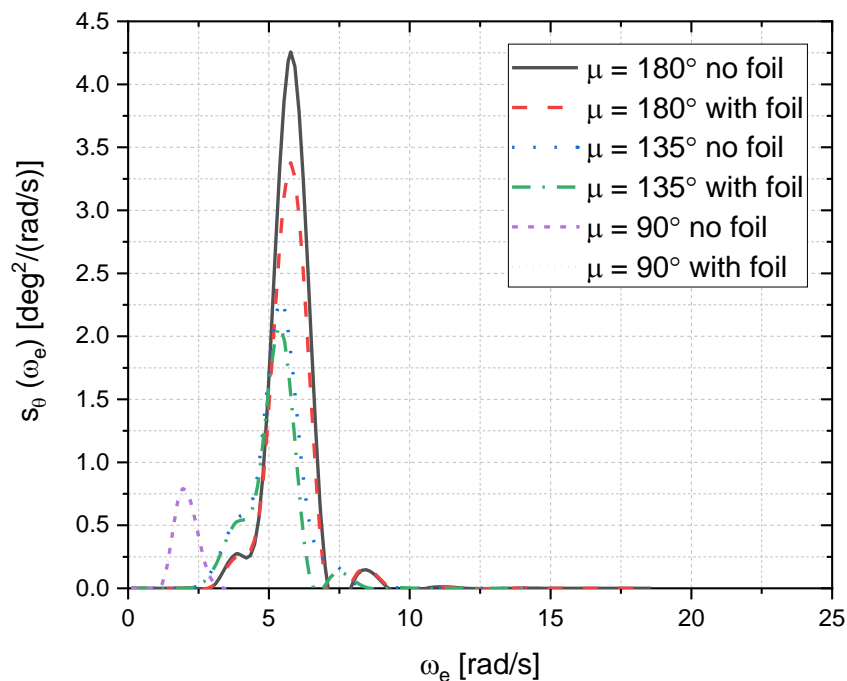


Fig. 16. Pitch spectra for catamaran with and without foil system at service speed $V_s = 24.5$ knots ($Fr = 1.24$) in sea state 2 ($H_s = 0.5$ m)

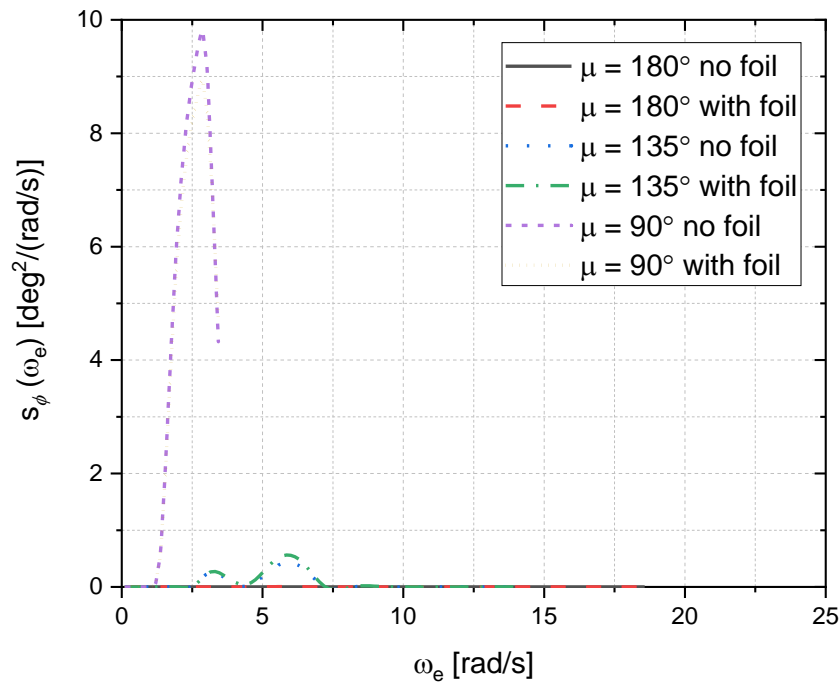


Fig. 17. Roll spectra for catamaran with and without foil system at service speed $V_s = 24.5$ knots ($Fr = 1.24$) in sea state 2 ($H_s = 0.5$ m)

Table 6

Heave significant amplitude [m] in sea state 2 ($H_s = 0.5$ m) for vessel's speed $V_s = 24.5$ knots

Heading angle μ	No foil system	With foil system	Difference [%]
180°	0.310	0.296	-4.41
135°	0.266	0.257	-3.25
90°	0.185	0.182	-2.13

Table 7

Pitch significant amplitude [deg] in sea state 2 ($H_s = 0.5$ m) for vessel's speed $V_s = 24.5$ knots

Heading angle μ	No foil system	With foil system	Difference [%]
180°	4.972	4.476	-9.97
135°	4.040	3.651	-9.63
90°	1.783	1.735	-2.70

Table 8

Roll significant amplitude [deg] in sea state 2 ($H_s = 0.5$ m) for vessel's speed $V_s = 24.5$ knots

Heading angle μ	No foil system	With foil system	Difference [%]
180°	Negligible	Negligible	
135°	1.917	2.178	13.64
90°	7.462	7.215	-3.30

4.3 Operability Analysis

To evaluate the seakeeping quality, the seakeeping performance of the vessel was checked against the NORDFORSK criteria for fast small crafts [12]. The criteria are tabulated in Table 9. To calculate the vertical accelerations at FP and at deck, it is necessary to obtain the relative motion and

vertical acceleration spectra in these locations (see Eq. (5) and Eq. (7)). The relative motion and vertical acceleration spectra at the deck in sea state 2 are shown in Figure 18 and Figure 19, respectively.

Table 9
NORDFORSK seakeeping criteria for fast small craft [12]

Description	Criteria
RMS of vertical acceleration at FP	$\leq 0.65 g$
RMS of vertical acceleration at deck	$\leq 0.275 g$
RMS of Roll	$\leq 4 \text{ deg}$

g is the gravitational acceleration = 9.81 m/s^2

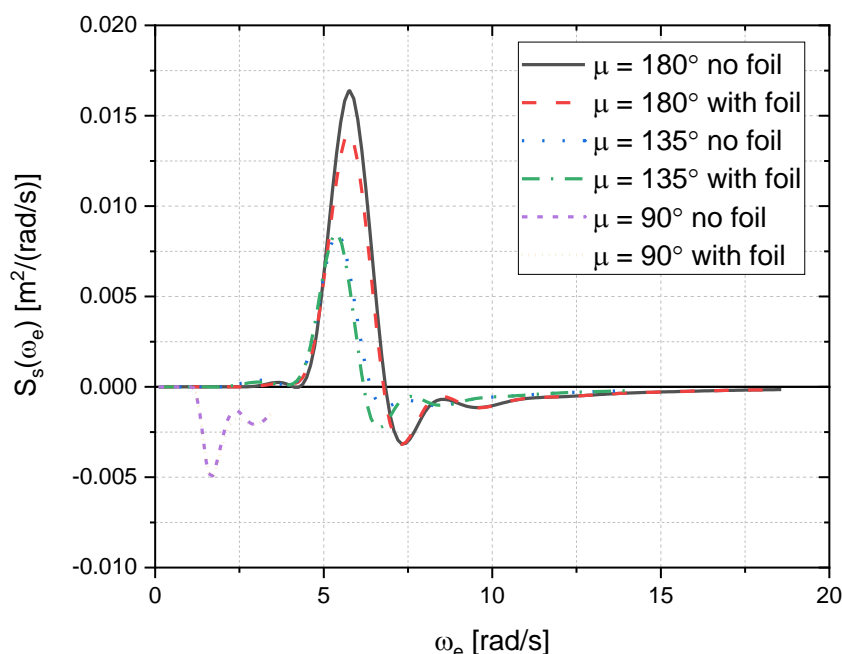


Fig. 18. Relative motion spectrum at the deck in sea state 2 ($H_s = 0.5 \text{ m}$) with $V_s = 24.5 \text{ knots}$ ($Fr = 1.24$)

The rms values of the vertical accelerations at FP and at deck, as well as the rms value of the roll motion, were calculated for sea states 2 and 3 ($H_s = 0.5$ and 1.25 m , respectively). Table 10 to Table 13 show that the seakeeping performance of the vessel passes the NORDFORSK criteria in sea state 2 but it fails in sea state 3. Table 10 to Table 13 also show that the vertical accelerations at FP and at deck were reduced due to the application of the foil system with a maximum decrease of 3.66 and 9.70 percent at FP and at deck, respectively, for wave heading $\mu = 180^\circ$. These results are consistent with those reported by Arii *et al.*, [7].

Table 10

Verification of the seakeeping performance against the NORDFORSK criteria for the case of catamaran without foil system in sea state 2 ($H_s = 0.5 \text{ m}$)

Description	Heading angle μ			Criteria	Status
	180°	135°	90°		
RMS of vertical acceleration at FP [m/s^2]	6.085	2.397	0.402	$\leq 0.65 g = 6.377$	OK
RMS of vertical acceleration at deck [m/s^2]	2.588	2.287	0.428	$\leq 0.275 g = 2.698$	OK
RMS of Roll [deg]	0.026	0.958	3.731	≤ 4	OK

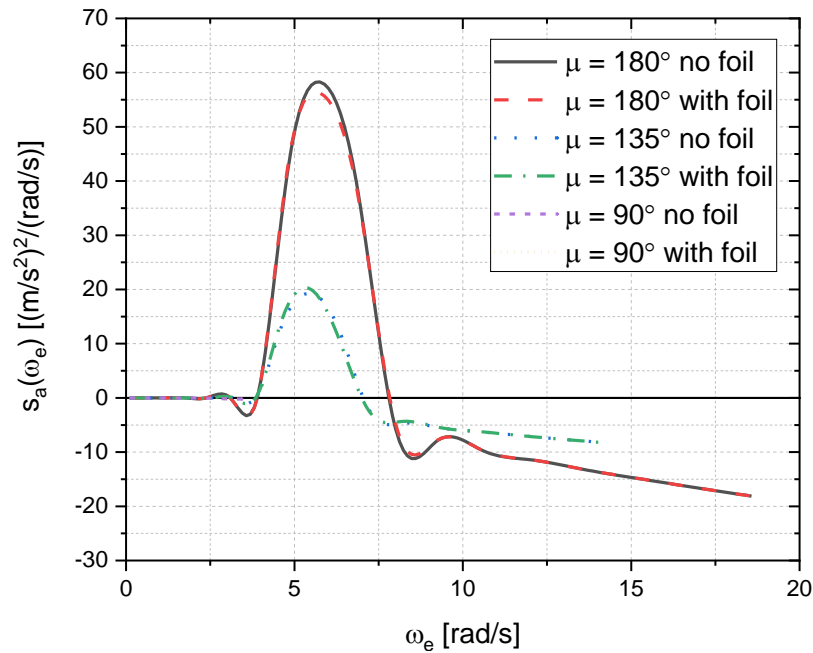


Fig. 19. Vertical acceleration spectrum at the deck in sea state 2 ($H_s = 0.5$ m) with $V_s = 24.5$ knots ($Fr = 1.24$)

Table 11

Verification of the seakeeping performance against the NORDFORSK criteria for the case of catamaran with foil system in sea state 2 ($H_s = 0.5$ m)

Description	Heading angle μ			Criteria	Status
	180°	135°	90°		
RMS of vertical acceleration at FP [m/s^2]	5.862	2.310	0.397	$\leq 0.65 g = 6.377$	OK
RMS of vertical acceleration at deck [m/s^2]	2.337	2.216	0.427	$\leq 0.275 g = 2.698$	OK
RMS of Roll [deg]	0.075	1.089	3.608	≤ 4	OK

Table 12

Verification of the seakeeping performance against the NORDFORSK criteria for the case of catamaran without foil system in sea state 3 ($H_s = 1.25$ m)

Description	Heading angle μ			Criteria	Status
	180°	135°	90°		
RMS of vertical acceleration at FP [m/s^2]	9.229	4.923	0.710	$\leq 0.65 g = 6.377$	FAILED
RMS of vertical acceleration at deck [m/s^2]	6.438	4.871	0.725	$\leq 0.275 g = 2.698$	FAILED
RMS of Roll [deg]	0.044	2.593	5.131	≤ 4	FAILED

Table 13

Verification of the seakeeping performance against the NORDFORSK criteria for the case of catamaran with foil system in sea state 3 ($H_s = 1.25$ m)

Description	Heading angle μ			Criteria	Status
	180°	135°	90°		
RMS of vertical acceleration at FP [m/s^2]	9.067	4.855	0.709	$\leq 0.65 g = 6.377$	FAILED
RMS of vertical acceleration at deck [m/s^2]	6.318	4.838	0.725	$\leq 0.275 g = 2.698$	FAILED
RMS of Roll [deg]	0.126	2.670	4.968	≤ 4	FAILED

5. Conclusions

A foil system was applied to an existing catamaran to improve the seakeeping performance of the vessel. This configuration of catamaran with foil system is referred to as hydrofoil supported watercraft (hysuwac). CFD simulations based on a panel method were carried out to obtain the seakeeping characteristics of the vessel in a seaway. Simulation results show that the foil system reduced the vessel motions at the service speed: the significant heave-, pitch- and roll amplitudes were reduced 4.41, 9.97 and 3.30 percent, respectively, due to the application of the foil system. Further, the vertical accelerations at the fore perpendicular (FP) and at deck were reduced 3.66 and 9.70 percent, respectively. These results are consistent with those reported in the literature. A check against the NORDFORSK criteria for fast small crafts shows that the vessel can operate safely in sea state 2. However, it cannot comply with the NORDFORSK criteria in sea states higher than 2.

Acknowledgements

The authors thank Mr. Eddy Noer Seto at PT. Maju Bangkit Indonesia Group, Surabaya, Indonesia, for providing the vessel's data and for the fruitful collaboration. The authors gratefully acknowledge the financial support from the Institut Teknologi Sepuluh Nopember (ITS), Surabaya, Indonesia, for this work, under project scheme of the Publication Writing and IPR Incentive Program (PPHKI).

References

- [1] Yun, Liang, Alan Bliault, and Huan Zong Rong. *High speed catamarans and multihulls: technology, performance, and applications*. Springer, 2018. <https://doi.org/10.1007/978-1-4939-7891-5>
- [2] Welnicki, Wieslaw. "The enhancement of seakeeping qualities of fast catamaran by means of stabilizing foils." *Polish Maritime Research* 3 (1998): 10-13.
- [3] Hoppe, K. G. "Optimisation of hydrofoil-supported planing catamarans." *Fast Sea Transportation* (1995).
- [4] Hoppe, K. G. "Recent applications of hydrofoil-supported-catamarans." *Fast Ferry International* 36 (2001).
- [5] Hoppe, K. G. "Boats, Hydrofoil Assisted Catamaran." *SA Patent* 80 (1980): 5400.
- [6] Hoppe, K. G. "Boats, Hydrofoil Supported Catamaran." *SA Patent* 82 (1982): 3505.
- [7] Arii, T., H. Yamato, T. Takai, and R. Shigehiro. "Development of a Motion Control System for a Foil-Assisted Catamaran 'Superjet-30'." In *Proceedings of the 2nd International Conference on Fast Sea Transportation (FAST'93)*, Volume 1, pp. 295–316, December 1993. Yokohama, Japan, 1993.
- [8] Najafi, Amin, Hashem Nowruz, and Hassan Ghassemi. "Performance prediction of hydrofoil-supported catamarans using experiment and ANNs." *Applied Ocean Research* 75 (2018): 66-84. <https://doi.org/10.1016/j.apor.2018.02.017>
- [9] Suastika, Ketut, Affan Hidayat, and Soegeng Riyadi. "Effects of the application of a stern foil on ship resistance: A case study of an Orela crew boat." *International Journal of Technology* 8, no. 7 (2017): 1266-1275. <https://doi.org/10.14716/ijtech.v8i7.691>
- [10] Riyadi, Soegeng, and Ketut Suastika. "Experimental and Numerical Study of High Froude-number Resistance of Ship Utilizing a Hull Vane®: A Case Study of a Hard-chine Crew Boat." *CFD Letters* 12, no. 2 (2020): 95-105.
- [11] Hoppe, Karl-Gunther W. "Catamaran with hydrofoils." *U.S. Patent* 4,606,291, issued August 19, 1986.
- [12] NORDFORSK. *Assessment of Ship Performance in a Seaway*. Copenhagen, Nordforsk, 1987.
- [13] Saputro, Slamet Agus, and Ketut Suastika. "Kajian eksperimental pengaruh posisi perletakan hydrofoil pendukung terhadap hambatan kapal." *Jurnal Teknik ITS* 1, no. 1 (2012): G51-G54.
- [14] Abbott, Ira H., and Albert E. Von Doenhoff. *Theory of wing sections: including a summary of airfoil data*. Courier Corporation, 2012.
- [15] Loveday, Howard. "The design of a hydrofoil system for sailing catamarans." *PhD diss., Stellenbosch: University of Stellenbosch*, 2006.
- [16] Nadapdap, Gilbert Ebenezer, Muhammad H. N. Aliffrananda, Yuda A. Hermawan, and Ketut Suastika. "Effects of the application of hydrofoils on the resistance of a catamaran: a case study of catamaran passenger ship." *The 4th World Virtual Conference on Applied Sciences and Engineering Applications in conjunction with the 6th International Symposium on Fluid Mechanics and Thermal Sciences (4th WVCASEA & 6th IS-FMITS) 2021, Malaysia* (2021).
- [17] BMKG. "Weather Forecast." *Indonesian Agency for Meteorology, Climatology and Geophysics*. Accessed on May 20, 2021. <https://www.bmkg.go.id/cuaca/prakiraan-cuaca-indonesia.bmkg?lang=EN>

-
- [18] ITTC. "Recommended Procedures and Guidelines - Seakeeping Experiments." *International Towing Tank Conference*, 2014.
- [19] Bhattacharyya, Rameswar. *Dynamics of marine vehicles*. John Wiley & Sons Incorporated, 1978.
- [20] Ansys Aqwa. "Ansys Aqwa Theory Manual." *Ansys, Inc., Canonsburg*, 2019.
- [21] Bentley. "Maxsurf Modeler User Manual." *Bentley System, Inc.*, 2015.